

Chapter 1

The initial conditions of star formation: cosmic rays as the fundamental regulators

Padelis P. Papadopoulos and Wing-Fai Thi

Abstract Cosmic rays (CRs) control the thermal, ionization and chemical state of the dense H_2 gas regions that otherwise remain shielded from far-UV and optical stellar radiation propagating through the dusty ISM of galaxies. It is in such CR-dominated regions (CRDRs) rather than Photon-dominated regions (PDRs) of H_2 clouds where the star formation initial conditions are set, making CRs the ultimate star-formation feedback factor in galaxies, able to operate even in their most deeply dust-enshrouded environments. CR-controlled star formation initial conditions naturally set the stage for a near-invariant stellar Initial Mass Function (IMF) in galaxies as long as their average CR energy density U_{CR} permeating their molecular ISM remains within a factor of ~ 10 of its Galactic value. Nevertheless, in the extreme environments of the compact starbursts found in merging galaxies, where $U_{\text{CR}} \sim (\text{few}) \times 10^3 U_{\text{CR,Gal}}$, CRs dramatically alter the initial conditions of star formation. In the resulting extreme CRDRs H_2 cloud fragmentation will produce far fewer low mass ($< 8 M_{\odot}$) stars, yielding a top-heavy stellar IMF. This will be a generic feature of CR-controlled star-formation initial conditions, lending a physical base for a bimodal IMF during galaxy formation, with a top-heavy one for compact merger-induced starbursts, and an ordinary IMF preserved for star formation in isolated gas-rich disks. In this scheme the integrated galactic IMFs (IGIMF) are expected to be strong functions of the star formation history of galaxies. Finally the large, CR-induced, ionization fractions expected for (far-UV)-shielded H_2 gas in the CRDRs of compact starbursts will lengthen the ambipolar diffusion (AD) timescales so much as to render the alternative AD-regulated rather (Jeans mass)-driven star formation scenario as utterly unrealistic for the ISM in such galaxies.

Padelis P. Papadopoulos

Max Planck Institute for Radioastronomy, Auf dem Huegel 69, D-5312, Bonn, Germany,
e-mail: padelis@mpifr-bonn.mpg.de

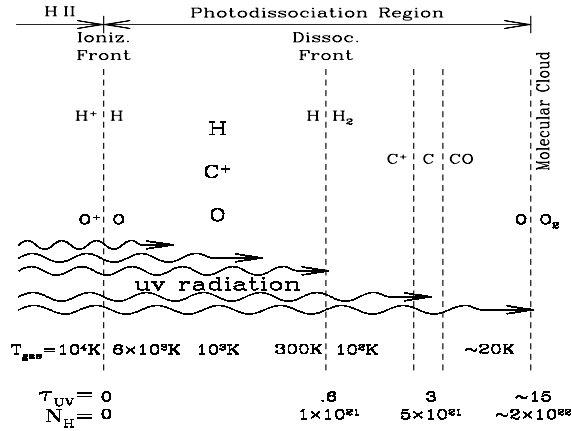
Wing Fai-Thi

UJF-Grenoble 1 / CNRS-INSU, Institut de Plantologie et d'Astrophysique (IPAG) UMR 5274,
38041, Grenoble, France,
e-mail: wing-fai.thi@obs.ujf-grenoble.fr

1.1 Cosmic rays versus far-UV and optical photons

Much of the interstellar medium (ISM) in galaxies resides in the so-called Photon-dominated regions (PDRs) where stellar far-UV photons ($6\text{ eV} < h\nu < 13.6\text{ eV}$) determine the thermal, ionization and chemical state of atomic (HI) and molecular (H_2) hydrogen gas [1]. For HI these phases are the Warm Neutral Medium (WNM, with $T_{\text{kin}} \sim 10^4\text{ K}$ and $n \sim (0.1\text{--}1)\text{ cm}^{-3}$) and the Cold Neutral Medium (CNM, with $T_{\text{kin}} \sim (80\text{--}200)\text{ K}$ and $n \sim (10\text{--}100)\text{ cm}^{-3}$) [2]. For the molecular PDRs in H_2 clouds on the other hand: $n \sim (10^2\text{--}10^6)\text{ cm}^{-3}$ and $T_{\text{kin}} \sim (30\text{--}100)\text{ K}$. Such PDRs start from the surface of molecular clouds (MCs) with a layered distribution (Fig. 1.1) of atomic and ionized species on the outside (HI , C^+ , C , O), and continue deep inwards where molecules such as CO dominate [3, 4], marking the location of such clouds via their mm/submm rotational line emission. The thermal, ionization, and chemical state of all these phases is determined by the far-UV photons whose influence, especially on the ISM chemistry, can extend very deep inside the low-density MCs ($n(\text{H}_2) \sim (100\text{--}500)\text{ cm}^{-3}$) typical in the Galaxy. The dust in PDRs is heated via absorption of the ambient far-UV and optical radiation and cools via continuum thermal IR/submm emission while the gas is heated via electrons ejected by the photoelectric effect on the concomitant dust grains and polycyclic aromatic hydrocarbons (PAHs). Despite the gas receiving $\sim 10^2\text{--}10^3$ less heating per unit volume than the dust, in PDRs it is always $T_{\text{kin}} > T_{\text{dust}}$. This is because of the much less efficient cooling of the gas via spectral lines while dust cools via continuum radiation across a wide range of wavelengths (typically peaking at IR/submm wavelengths). Turbulent heating of the gas in MCs will further reinforce the $T_{\text{kin}} > T_{\text{dust}}$ inequality, since it does not involve the dust reservoir.

Fig. 1.1 The structure of a typical PDR/CRDR. Atomic and ionized species reside on the (far-UV)-illuminated outer parts (left) while neutral atoms (O) and molecules such as CO dominate deeper inside, the domain of CRDRs and CR-controlled thermal and chemical gas states.



For MCs in the typical ISM conditions of spiral disks where $\langle A_V \rangle \sim 3\text{--}7$ (in units of optical extinction), there can only be very little H_2 gas residing in their dense (far-UV)/optical-shielded regions. Its mass fraction per MC is $\sim (1\text{--}5)\%$, a census found

from surveys of CO J=1–0 (total H₂ mass indicator) and rotational transitions of dense gas tracer molecules such as the HCN (mostly J=1–0), and using the HCN/CO line ratio to determine $f_{\text{dense}} = M(n \geq 10^4 \text{ cm}^{-3}) / M_{\text{tot}}(\text{H}_2)$ [6, 5]. Here is important to note that the more complex heavy rotor molecules such as HCN will necessarily trace the dense but also (mainly) the (far-UV)-shielded mass of MCs since, unlike H₂ and its tracer molecule CO, they have much lower dissociation potentials (~ 5 eV for HCN versus ~ 13 eV for H₂, and ~ 10 eV for CO).

Simple approximate estimates of the mass fraction contained in the PDRs of (far-UV)-irradiated MCs can be found by computing the mass of outer atomic HI layer marking the HI→H₂ transition, itself comparable to the mass of the warm PDR H₂ gas layer extending further inwards. Thus the PDR-residing gas column density (HI and H₂) will be $\sim 2 \times N_{\text{tr}}(\text{HI})$. The latter can be computed for a given radiation field G_0 (in Habing units), metallicity Z ($Z=1$ being solar), average gas density n , and an H₂ formation rate R_f . In units of optical extinction this transition layer is ([9]):

$$A_v^{(\text{tr})} = 1.086 \xi_{\text{FUV}}^{-1} \ln \left[1 + \frac{G_0 k_0}{n R_f} \Phi \right] \quad (1.1)$$

where $k_0 = 4 \times 10^{-11} \text{ s}^{-1}$ is the H₂ dissociation rate (for $G_0=1$), $R_f \sim 3 \times 10^{-17} \text{ cm}^{-3} \text{ s}^{-1}$ its formation rate on grains (for typical CNM HI), and $\Phi = 6.6 \times 10^{-6} \sqrt{\pi} Z^{1/2} \xi_{\text{FUV}}$ is the H₂ self-shielding function integrated over the HI/H₂ transition layer, with $\xi_{\text{FUV}} = \sigma_{\text{FUV}} / \sigma_v \sim 2-3$ being the dust cross section ratio for far-UV and optical light. Using existing formalism ([9]) the PDR-related gas mass fraction per MC then is:

$$f_{\text{PDR}} \sim 2 \times \left[1 - \left(1 - \frac{4 A_v^{(\text{tr})}}{3 \langle A_v \rangle} \right)^3 \right], \quad (1.2)$$

assuming spherical and uniform MCs that do not cross-shield and hence each receives the full (far-UV)/optical radiation field, assumptions that make the computed f_{PDR} a maximum. The average optical extinction $\langle A_v \rangle$ per MC is of course finite and a function of the ambient ISM conditions, mainly the gas pressure (dominated by supersonic non-thermal rather than thermal velocity fields). Expressing an empirical Galactic (average MC density)-(size) relation: $n \propto (2R)^{-1}$, along with its expected normalization in terms of cloud boundary pressure P_e ([9]) in terms of average optical extinction yields:

$$\langle A_v \rangle \sim 0.22 Z \frac{n_0}{100 \text{ cm}^{-3}} \left(\frac{P_e / k_B}{10^4 \text{ cm}^{-3} \text{ K}} \right)^{1/2}, \quad (1.3)$$

where $n_0 \sim 1500 \text{ cm}^{-3}$. For average MC densities of $\sim 100 \text{ cm}^{-3}$, Solar metallicities, $\xi_{\text{FUV}}=2$, and $G_0=5-10$ (for typical star-forming gas) Equation 1.1 yields $A_v^{(\text{tr})} \sim 0.50-0.75$, while for typical interstellar pressures in galactic disks $P_e / k_B \sim (1-2) \times 10^4 \text{ K cm}^{-3}$ it would be $\langle A_v \rangle \sim 3.3-4.7$. The latter is the A_v range over which the abundance of C⁺ plummets, giving rise to C and CO while the free electron abundance is much reduced (see Fig. 1.2).

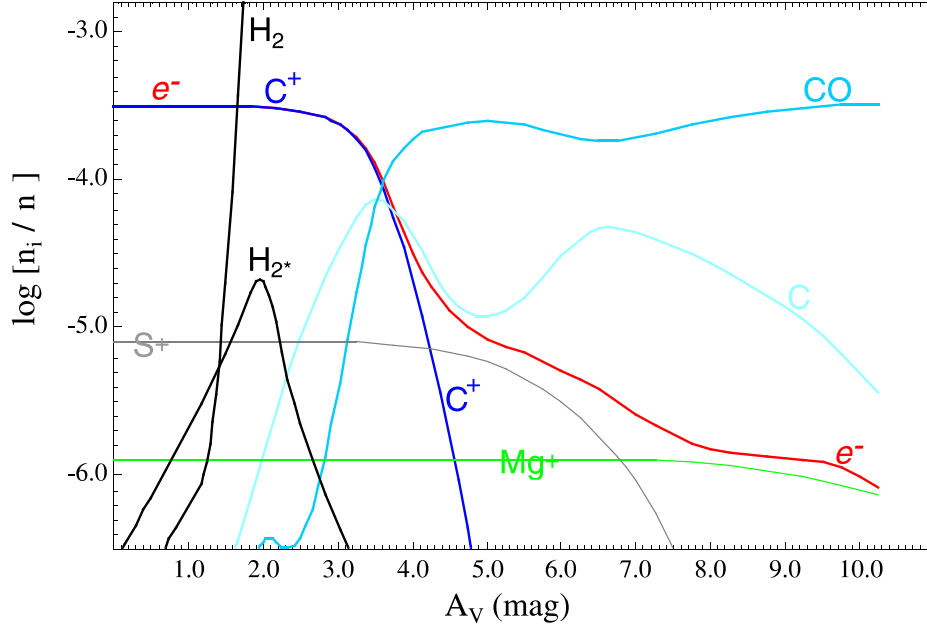


Fig. 1.2 The PDR→CRDR transition zone as marked by the rapidly decreasing C^+ and e^- abundances deep inside a (far-UV)-illuminated molecular cloud (radiation field incoming from the left). Note the dramatic fall of the electron abundance beyond $A_V \sim 4$.

For the finite MCs this outer HI/(warm H_2) PDR gas still contains $f_{\text{PDR}} \sim 0.74$ –1 of their mass (from Equation 1.2), i.e. *most of the HI and H_2 gas in typical star-forming ISM environments resides in PDRs*. Later we will see that this will not be so in the high-pressure ISM of Ultra Luminous Infrared galaxies (ULIRGs), merger systems with very IR-luminous ($L_{\text{IR}} \geq 10^{12} L_{\odot}$) compact starbursts (Sect. 1.4).

1.2 The physical conditions of the gas: PDRs versus CRDRs

The wide range of physical conditions of the HI and H_2 gas in PDRs (Sect. 1.1) is the direct result of: a) the widely varying strengths of the dust-absorbed far-UV and optical radiation (and thus of the gas photoelectric heating per H, and dust heating) within the PDRs, and b) the large range of densities (and thus of the cooling power per H) that are expected in the supersonically turbulent MCs ([7]). Dissipation of the supersonic turbulence via shocks ([8]) will further contribute to the wide range of temperatures observed in the PDR-residing gas of MCs. Moreover their average electron abundance $x(e) = n_e / [2n(H_2)]$ changes by ~ 2 –3 orders of magnitude, starting from a maximum of $\sim 3 \times 10^{-4}$ (that corresponds to a fully ionized carbon).

The dense gas cores ($n \sim (10^5 - 10^6) \text{ cm}^{-3}$) in Galactic CRDRs on the other hand span a much narrower range of temperatures and ionization states, with $\langle T_{\text{kin}} \rangle \sim 10 \text{ K}$ (and $\sim 30\%$ dispersion), and $x(e) \sim (\text{few}) \times 10^{-8}$ (varying by less than a factor of ~ 5). These CRDR conditions, widely observed in the Galaxy ([10], [11]), are a result of a nearly complete lack of far-UV and optical photons in such regions (thus no photoelectric gas heating or strong dust heating), nearly complete dissipation of supersonic gas motions ([12]), and the onset of strong gas-dust thermal coupling setting $T_{\text{kin}} \sim T_{\text{dust}}$. This simply means that cold dust grains inside CRDRs, warmed only by the feeble IR radiation able to leak inside them, can now act as powerful ‘thermostats’ of the H_2 gas. The latter is now heated almost exclusively by primary and secondary ionizations induced by low-energy CRs ($10 \text{ MeV} \leq E_{\text{CR}} \leq 100 \text{ MeV}$) [13] which, unlike far-UV and optical photons, penetrate deep inside such regions, and thus *fully regulate their thermal, ionization and chemical states*.

The aforementioned CR-controlled dense H_2 gas states in ordinary star-forming environments is expected also on broad theoretical grounds, namely: a) high density gas regions will be typically nested well inside less dense gas structures of supersonic MCs [14], and thus will always ‘see’ a much-attenuated stellar radiation field, b) high-density gas is also strongly cooling gas (since $(\text{line-cooling}) \propto [n(\text{H}_2)]^2$), and c) turbulent energy injected on the largest gas structures with low average densities $\sim (10 - 10^3) \text{ cm}^{-3}$ will have fully dissipated in the high density gas of CRDRs. It is actually these three reasons, along with the strong thermal coupling of the gas in CRDRs to a necessarily cold dust (for lack of far-UV/optical photons) reservoir, that *make it very difficult for large masses of warm and dense H_2 gas to exist in ordinary star-forming galaxies*. Finally, as already mentioned in 1.1, only few% of the total H_2 gas mass resides at such high densities anyway, as expected also from MC simulations ([7]) under conditions found in ordinary star-forming spiral disks.

1.2.1 Computing T_{kin} and $x(e)$ in CRDRs: a simpler method

In CRDRs the $T_{\text{kin}}^{(\text{min})}$ and $x_{\text{min}}(e)$ minimum values expected for H_2 gas in galaxies are set. However determining them involves solving the coupled equations of thermal, chemical and ionization balance in such regions since CRs heat the gas but also affect the abundance of various molecular and atomic coolants. We can nevertheless make some simplifying assumptions that will keep the physics involved transparent while demonstrating the range of $T_{\text{kin}}^{(\text{min})}$ and $x_{\text{min}}(e)$. Following standard methods ([15]) $T_{\text{kin}}^{(\text{min})}$ in CRDRs can be computed by solving the equation of thermal balance:

$$\Gamma_{\text{CR}} = \Lambda_{\text{line}} + \Lambda_{\text{g-d}}, \quad (1.4)$$

where $\Gamma_{\text{CR}} \propto \zeta_{\text{CR}} n(\text{H}_2)$ is the CR heating with $\zeta_{\text{CR}} \propto U_{\text{CR}}$ being the CR ionization rate, and U_{CR} the average CR energy density. For $T_{\text{kin}} \leq 50 \text{ K}$ (which encompasses what is expected for CRDRs of ordinary star-forming galaxies), the line cooling term Λ_{line} is dominated by CO lines. However for the much more extreme CRDRs

expected in ULIRGs, higher temperatures are possible and thus cooling from the atomic fine structure lines O I (at $63 \mu\text{m}$) and C^+ (at $158 \mu\text{m}$) can become important. The C^+ abundance in CRDRs is not necessarily negligible as it is no longer controlled by a stellar far-UV radiation field (as in PDRs), but by ISM-CR interactions inducing internal UV radiation which destroys CO and produces C^+ , a clear demonstration of the coupled thermal and chemical states of the gas in CRDRs. Finally the term $\Lambda_{\text{g-d}}$ denotes the all-important (in CRDRs) cooling of the gas via the gas-dust coupling which depends on the gas and dust temperatures. Thus the thermal balance equation becomes

$$\Lambda_{\text{CO}}(T_{\text{kin}}) + \Lambda_{\text{g-d}}(T_{\text{kin}}, T_{\text{dust}}) + \Lambda_{\text{OI63}}(T_{\text{kin}}) + \Lambda_{\text{C}^+}(T_{\text{kin}}) = \Gamma_{\text{CR}}, \quad (1.5)$$

(see the Appendix for the detailed expressions used). We have not considered turbulent gas heating since we want to compute the minimum CR-controlled gas temperatures and since supersonic turbulence (and thus shock-heating) has typically dissipated in the dense pre-stellar gas regions inside CRDRs.

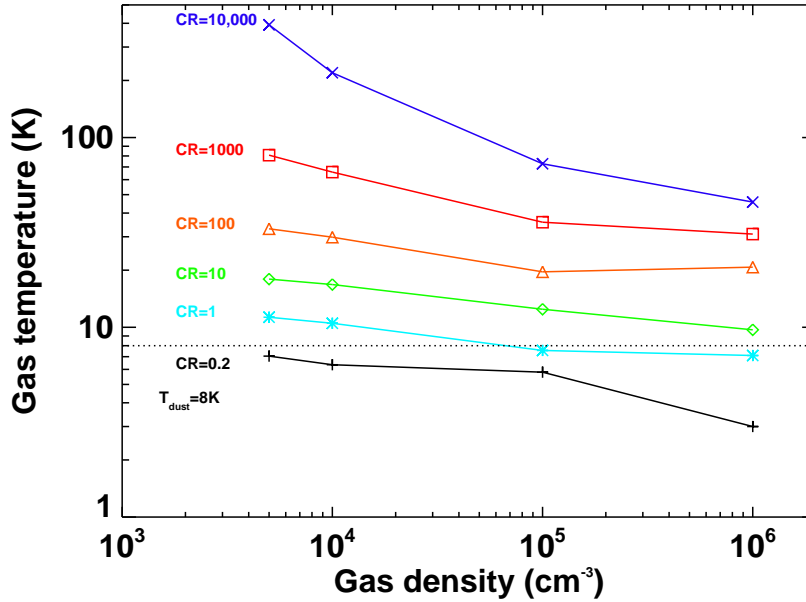


Fig. 1.3 The equilibrium temperature of (far-UV)-shielded regions in CRDRs computed from equation 1.5. The CR energy densities range from those expected in ordinary star-forming environments Galaxy [$U_{\text{CR}}=(0.2-10) \times U_{\text{CR,Gal}}$] to those expected in the extreme CRDRs of ULIRGs [$U_{\text{CR}}=(10^2-10^4) \times U_{\text{CR,Gal}}$]. A dust temperature of $T_{\text{dust}}=8 \text{ K}$, and a Galactic CR ionization rate of $\zeta_{\text{CR}}=5 \times 10^{-17} \text{ s}^{-1}$ have been assumed.

In order to solve the gas thermal balance equation in principle we also must solve for T_{dust} in CRDRs. For the purposes of computing $T_{\text{kin}}^{(\text{min})}$ we set $T_{\text{dust}}=8$ K, which is typical for CR-dominated cores in the Galaxy. Any stronger IR radiation field leaking inside such cores (as expected in starbursts) or remnant turbulent gas heating can only raise the gas temperatures computed here. In Fig. 1.3 the $T_{\text{kin}}^{(\text{min})}$ values show that CR-heated dense gas ($>10^4 \text{ cm}^{-3}$) remains cold ($\sim(10\text{-}15)$ K) for U_{CR} within $\sim(0.2\text{-}10) \times U_{\text{CR,Gal}}$, rising decisively only when $U_{\text{CR}} \sim (\text{few}) \times 10^3 U_{\text{CR,Gal}}$ where the thermal balance equation yields $T_{\text{kin}}^{(\text{min})} \sim (40\text{-}100)$ K.

Solving for the coupled chemical and thermal states of dense gas in CRDRs does not change much of the aforementioned picture while it makes clear another important aspect that of CR-controlled thermal states of the gas, namely that high CR energy densities *will induce a strong gas-dust thermal decoupling*, with $T_{\text{kin}}^{(\text{min})}$ remaining significantly higher than T_{dust} , even at high gas densities (Fig. 1.4).

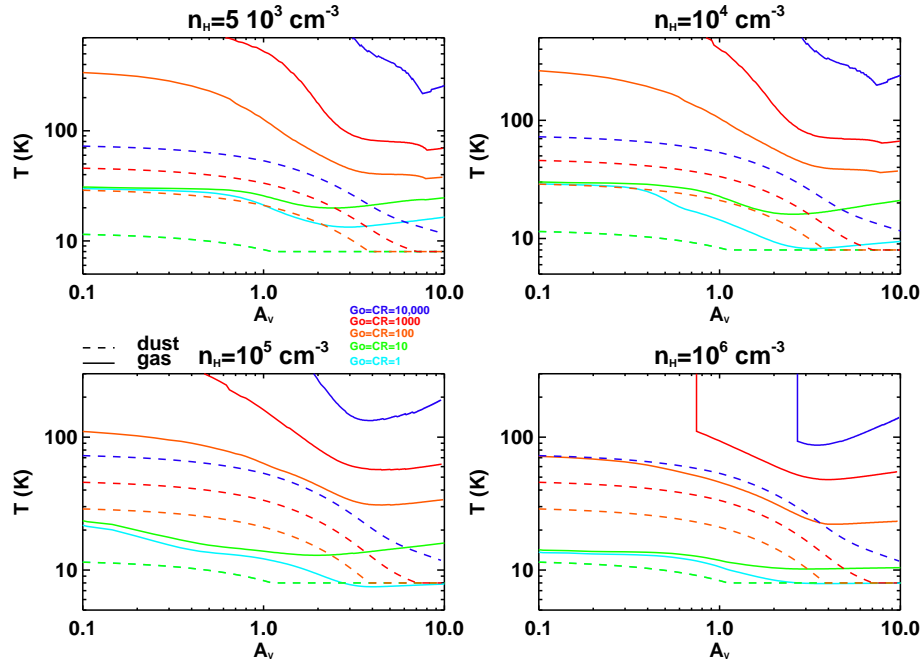


Fig. 1.4 The gas and dust temperature profiles (solid and dotted lines of similar color) versus optical extinction inside a molecular cloud. These were computed by solving the coupled thermal and chemical balance equations ([19]), while also assuming a far-UV radiation field (incident on the $A_v=0$ surface of plane clouds) that scales in an identical fashion as the average CR energy density pervading the H_2 cloud. Their common scaling runs as $(1, 10, 10^2, 10^3, 10^4) \times \text{Galactic}$. Unlike in Fig. 1.3 the dust is significantly warmed by the stronger (far-UV)/optical radiation fields absorbed by the outer cloud layers and the re-radiated dust IR emission that penetrates deeper into the cloud.

This happens even as the dust temperatures deep inside H_2 clouds rise because of an incident radiation that is now set to scale identically to the average CR energy density (both assumed proportional to the average star-formation rate density $\dot{\rho}_{sfr}$). This CR-induced thermal decoupling persists deep inside the cloud ($A_V=5-10$) even at the highest gas densities explored here where gas-dust thermal interaction will be the strongest. It must also be noted that for a given average $\dot{\rho}_{sfr}$ in a galaxy, the resulting gas-dust temperature inequality will likely be even larger since cross-shielding between H_2 clouds as well as dusty WNM and CNM HI gas interdispersed between such clouds will reduce the average radiation field incident on them, but not the deeply penetrating CRs. Thus while $U_{CR} \propto \dot{\rho}_{sfr}$, the scaling of average G_0 with $\dot{\rho}_{sfr}$ will be weaker than linear (unlike what was assumed in Fig. 1.4 for simplicity).

From Fig. 1.4 it can also be discerned that even for strongly boosted far-UV radiation fields, gas temperatures are solely CR-controlled and remain almost invariant with A_V beyond $A_V \sim 5$. This characteristic of CRDRs is of great importance when it comes to the initial conditions of star formation, and the near-invariant mass scale of the stellar IMF found in the Galaxy and ordinary star-forming galaxies.

An order of magnitude estimate of the CR-regulated equilibrium ionization fraction of (far-UV)-shielded gas can also be found without resorting to solving the full chemistry network involved. Following an analytical approach ([20]) yields

$$x(e) = 2 \times 10^{-7} r_{gd}^{-1} \left(\frac{n_{ch}}{2n(H_2)} \right)^{1/2} \left[\left(1 + \frac{n_{ch}}{8n(H_2)} \right)^{1/2} + \left(\frac{n_{ch}}{8n(H_2)} \right)^{1/2} \right] \quad (1.6)$$

where $n_{ch} \sim 500 \left(r_{gd}^2 \zeta_{-17} \right) \text{ cm}^{-3}$ is a characteristic density encapsulating the effects of cosmic ray ionization and ambient metallicity on the ionization balance (r_{gd} is the normalized gas/dust ratio $r_{gd} = [(G/D)/100]$ with G/D (gas-to-dust mass) = 100 for Solar metallicities. The main assumptions underlying the validity of Equation 1.6 are three, namely: a) all the gas is H_2 and all the carbon is locked in CO (so C^+ does not dominate the ionization), b) all negative charge is carried by the free electrons and molecular ions are destroyed mostly by recombination with these free electrons, and c) the metal abundance is small with respect to the heavy molecule abundance.

For the Galaxy ($\zeta_{CR, Gal} = 5 \times 10^{-17} \text{ s}^{-1}$) it is $n_{ch} = 2.5 \times 10^3 \text{ cm}^{-3}$, and for a typical dense core of $n(H_2) = 10^5 \text{ cm}^{-3}$ it would be $x(e)_{Gal} \sim 2.4 \times 10^{-8}$. A boost of ζ_{CR} by a factor of 10 yields $x(e) = 8.4 \times 10^{-8}$, retaining the low ionization fraction necessary for an ambipolar-diffusion regulated star-formation to proceed in such cores ([20]).

1.3 CRDRs and the star formation initial conditions in galaxies

CRDRs are the ISM regions where the initial conditions of star-formation are set. Thus their thermal and/or ionization state is expected to play a critical role on the emergence of the stellar IMF and its mass scale. This remains the case for both main

star formation scenaria proposed, namely: a) star formation driven by gravitational collapse of high overdensity peaks in supersonically turbulent H_2 clouds, and b) regulated by ambipolar-diffusion (AD) in dense cores whose low $x(e)$ allows the magnetic field lines to slip away making them supercritical (i.e. $M_{\text{core}}/M_\Phi > 1$ where $M_\Phi = 0.12\Phi/G^{1/2}$, and Φ is the magnetic field flux threading the cores, [21]) and able to collapse towards star formation. The only difference will be which CRDR gas property: the Jeans mass or $x(e)$, is important in determining the stellar IMF.

It is worth emphasizing that star formation initial conditions set in CRDRs naturally explain the first mystery regarding the stellar IMF, namely its near-universality in ordinary ISM environments. Indeed the large range of thermal, turbulent, and ionization states present for the H_2 gas phase in the Milky Way, makes the emergence of a near-universal stellar IMF an unlikely outcome even for the Galaxy if such states were all used as star formation initial conditions. The gas in CRDRs on the other hand, lying beyond the reach of varying far-UV radiation fields and turbulence-induced shock heating, with a near-isothermal state at $T_{\text{kin}} \sim T_{\text{dust}}$, near-thermal motions, and the lowest possible $x(e)$ values, is a natural choice of well-protected initial conditions of star formation that can then lead to a near-invariant stellar IMF mass scale. Similar arguments have been made in the past ([22]), but only recently it was demonstrated just how robust the cold thermal state of CRDRs remains irrespective of the average conditions prevailing at the outer boundaries of the MCs that contain them ([34]). Finally, as long as the average CR energy density pervading CRDRs remains within a factor of ~ 10 of its Galactic value, neither the temperature nor the ionization fraction within CRDRs changes substantially. This state of affairs is however dramatically altered in the compact, merger-induced starbursts found in ULIRGs.

1.4 CRDRs in compact starbursts: new initial conditions for star formation

Some of the most spectacular star formation events in the local and the distant Universe are found in strong galaxy mergers. In such systems tidal torques funnel the bulk of the molecular gas of their gas-rich disk progenitors into regions not much larger than the Galactic Center ([24]). There they settle into small ($2r \leq (100-300)\text{pc}$) and very turbulent H_2 gas disks, fueling extreme star-forming events ([25, 24]). The H_2 gas in ULIRGs, with one-dimensional Mach numbers of $M_{\text{ULIRGs}} \sim (5-30) \times M_{\text{spirals}}$, is expected to have larger mass fractions at densities of $> 10^4 \text{ cm}^{-3}$ ([8]), and this is indeed observed ([5, 6]).

However most of the large dense H_2 masses found in ULIRGs cannot reside in PDRs, a result of the high (turbulent) pressures ($P_e/k_B \sim 10^7 \text{ K cm}^{-3}$) and high gas densities in these galaxies. Indeed, from Equation 1.3 (and a Solar metallicity) such high gas pressures yield $\langle A_v \rangle \sim 100$, while for the high *average* gas densities of $\geq 10^4 \text{ cm}^{-3}$ typical for ULIRGs ([26]), it is $A_v^{(\text{tr})} \leq 2$ (Eq. 1.1) even for far-UV radiation fields as strong as $G_0 = 10^4$. Thus any warm gas mass fraction residing in

PDRs will be $\leq 15\%$ (Equation 1.2). In summary, while much larger dense gas mass fractions are expected and indeed observed in ULIRGs than in isolated star-forming gas-rich spirals, *most of their dense gas mass will not reside in PDRs*. Nevertheless recent observational results indicate large amounts of warm *and* dense gas in some ULIRGs, with average gas temperatures much larger than those deduced for the concomitant dust ([27]). Since a massive warm and dense H_2 phase cannot be in PDRs, far-UV/optical photons are inadequate energy suppliers of its observed state in ULIRGs. Only high CR energy densities (and/or strong turbulent heating) is capable of volumetrically heating the H_2 gas (unlike far-UV photons in PDRs) while also maintaining a significant $T_{\text{kin}} > T_{\text{dust}}$ inequality.

CR energy densities of $U_{\text{CR}} \sim [(\text{few}) \times 10^2 - 10^4] \times U_{\text{CR,Gal}}$ are expected in the compact starbursts found in ULIRGs ([29]) and, as indicated by Fig. 1.4, such high U_{CR} can easily maintain high gas temperatures while the concomitant dust remains much cooler. Such conditions have been inferred in the past for the Galactic Center ([30]) as well as for the center of NGC 253 ([31, 32]). However in the case of ULIRGs these conditions prevail over galaxy-size H_2 gas reservoirs that are ~ 2 -3 orders of magnitude more massive. Thus temperatures of $T_{\text{kin}} \sim (50-100)$ K are the new *minimum* values possible for gas in ULIRGs, and represent dramatically different initial conditions for star formation in their ISM environments.

The thermal state of dense gas in CRDRs is thus no longer a near-invariant but strongly altered by the high CR energy backgrounds expected in ULIRGs. In the so-called gravoturbulent H_2 cloud fragmentation scenario ([33]) this large temperature boost across a wide density range (Fig. 1.3) is expected to suppress low mass star formation. This is because the Jeans mass of the CR-heated gas in CRDRs,

$$M_{\text{Jeans}}^{(c)} = \left(\frac{k_B T_k}{G \mu m_{H_2}} \right)^{3/2} \rho_c^{-1/2} = 0.9 \left(\frac{T_k}{10\text{K}} \right)^{3/2} \left[\frac{n_c(H_2)}{10^4 \text{cm}^{-3}} \right]^{-1/2} M_{\odot}, \quad (1.7)$$

changes from $M_{\text{Jeans}}^{(c)} \sim 0.3 M_{\odot}$ for $n_c(H_2) = 10^5 \text{cm}^{-3}$, and $T_k = 10$ K (typical for the Galaxy) to $M_{\text{Jeans}}^{(c)} \sim (3-10) M_{\odot}$ for the same density and $T_k = (50-110)$ K expected to be the new minimum in the extreme CRDRs of ULIRGs. It is worth pointing out that an $M_{\text{Jeans}}^{(c)} \sim 0.3 M_{\odot}$ nicely matches the characteristics mass of the stellar IMF (the so-called IMF ‘knee’). Its observed near invariance under a wide range of ISM conditions (e.g. radiation fields) has been demonstrated theoretically ([34]), leaving CR energy densities *as the sole star-formation feedback mechanism that can decisively alter the initial conditions of star formation in galaxies*. This mechanism, driven by the massive stars (whose strong winds and explosive deaths provide the CR acceleration), will operate unhindered in the dusty ISM environments of extreme merger/starbursts (unlike photons), and it can reach where supersonic turbulence cannot, the small, dense and (far-UV)-shielded cores deep inside H_2 clouds.

In Fig. 1.5 the Jeans masses are shown for a density range encompassing that of typical star-forming H_2 clouds, demonstrating that for $U_{\text{CR}}/U_{\text{CR,Gal}} \geq 10^3$, M_{Jeans} increases by a factor of ~ 10 across the entire density range. This will invariably

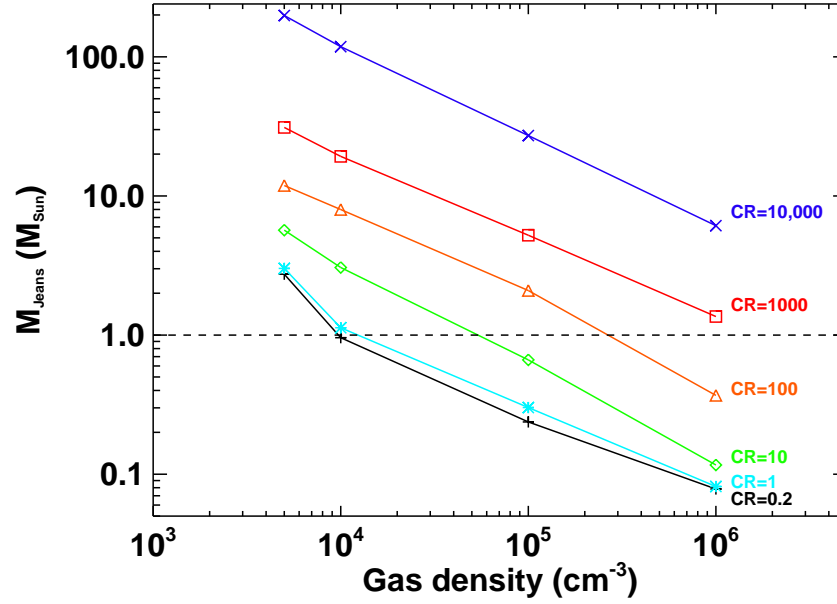


Fig. 1.5 The Jeans mass estimated from Equation 1.7 and the gas temperatures inside CRDRs, which were determined by solving the fully coupled thermal and chemical balance equations. The temperatures shown are averages of the $A_V=5-10$ part of the H_2 clouds where CR become dominant regulators of the gas thermal and chemical states (Fig. 1.4).

lead to higher characteristic mass $M_{\text{ch}}^{(*)}$ for newly formed stars, and thus a top-heavy stellar IMF ([22, 34]). For an $M_{\text{ch}}^{(*)} \sim M_{\text{Jeans}}(n_c)$ at the typical density of Galactic CRDR dense gas cores ($n_c \sim (\text{few}) \times 10^5 \text{ cm}^{-3}$) Fig. 1.5 also shows that variations of $U_{\text{CR}}/U_{\text{CR,Gal}} \sim 0.2-10$ would leave $M_{\text{ch}}^{(*)} \sim (0.3-0.5) M_{\odot}$ and still compatible with a standard stellar IMF. This is important since a larger sensitivity of $M_{\text{ch}}^{(*)}$ on U_{CR} would have been incompatible with its observed near-invariance in ordinary star-forming environments (where variations of the star-formation rate density $\dot{\rho}_{\text{sfr}}$, and thus of U_{CR} , by factors of $\sim 5-10$ are not extraordinary).

It must be noted that the choice of the particular (n, T_k) phase whose M_{Jeans} sets $M_{\text{ch}}^{(*)}$ is not without ambiguities even if some consensus has been established on the decisive role of $M_{\text{Jeans}}(\mathbf{r}, t)$ in driving the outcome of the gravoturbulent process at each spatial and temporal point (\mathbf{r}, t) . Arguments have been made both for $M_{\text{ch}}^{(*)} \propto \langle M_{\text{Jeans}} \rangle$ at the *onset* of a gravoturbulently driven MC fragmentation process ([33]), and for $M_{\text{ch}}^{(*)} \sim M_{\text{Jeans}}(n_c, T_k)$ at some characteristic gas density n_c . For gravoturbulent-regulated star-formation n_c is the density where efficient gas-dust thermal coupling of (far-UV)/optically-shielded gas lowers its temperature to the minimum value possible, i.e. that of $\sim T_{\text{dust}}$, rendering such gas regions nearly

isothermal. For the Galaxy this occurs at $n_c \sim 10^5 \text{ cm}^{-3}$, which is also similar to the density of regions where the transition from supersonically turbulent to near thermal gas motions occurs ([10, 22]).

For CRDRs with high average U_{CR} like those expected in compact starbursts, Fig. 1.4 makes obvious that gas-dust coupling is no longer adequate to lower T_{kin} to that of the concomitant dust for densities as high as 10^6 cm^{-3} . Thus a characteristic gas density can no longer be defined by the onset of thermal equilibrium between gas and dust in CRDRs, at least within the range of densities where appreciable amounts of mass can be found in ordinary MCs. This leaves the choice of $M_{\text{ch}}^{(*)} = M_{\text{Jeans}}(n_c, T_k)$ open, and thus it is worth examining the possible direction its value would take in extreme CRDRs. In the CR-innuded H_2 clouds inside compact starbursts n_c can now be set only as the typical density of regions where supersonic turbulence has fully dissipated and near-thermal motions dominate. The average density of such transition regions can be determined from two well-known scaling relations found for H_2 clouds: $\sigma_v(r) = \sigma_o (r/\text{pc})^h$ (linewidth-size) and $\langle n \rangle = n_o (r/\text{pc})^{-1}$ (density-size) after setting $\sigma_v(\text{min}) = (3k_B T_k / \mu m_{\text{H}_2})^{1/2}$ as the minimum linewidth possible, and solving for the corresponding mean density,

$$\langle n_c \rangle = n_o \left(\frac{\mu m_{\text{H}_2} \sigma_o^2}{3k_B T_k} \right)^{1/2h} \sim 11 n_o \left(\frac{\sigma_o}{\text{km s}^{-1}} \right)^2 \left(\frac{T_k}{10\text{K}} \right)^{-1}. \quad (1.8)$$

For $h=1/2$ (expected for pressurized H_2 virialized clouds [35]), $\sigma_o = 1.2 \text{ km s}^{-1}$ and $n_o = (\text{few}) \times 10^3 \text{ cm}^{-3}$ (from observations), it is $\langle n_c \rangle \sim (\text{few}) \times 10^4 \text{ cm}^{-3}$. For the CR-boosted $T_{\text{kin}}(\text{min})$ of extreme CRDRs $T_k(\text{min}) \sim (50-100) \text{ K}$: $\langle n_c \rangle \sim \text{few} \times 10^3 \text{ cm}^{-3}$. Thus the (turbulent gas) \rightarrow (thermal core) transition in extreme CRDRs will occur at lower densities *as well as* higher (CR-boosted) T_{kin} values than in ordinary Galactic ones. This will then shift a $M_{\text{ch}}^{(*)} \sim M_{\text{Jeans}}(n_c, T_k)$ both vertically (higher T_{kin}), as well as to the left (lower $n(\text{H}_2)$) of Fig. 1.5, yielding even higher $M_{\text{ch}}^{(*)}$ values than those resulting from only a vertical shift of M_{Jeans} because of CR-boosted gas temperatures. Thus irrespective of the H_2 cloud fragmentation details, and as long as the Jeans mass plays a decisive role in it, *a much larger characteristic mass $M_{\text{ch}}^{(*)}$ is expected for stars forming in the CRDRs of extreme starbursts.*

1.4.1 Ambipolar-diffusion regulated star formation

The CR-induced boost of the ionization fraction $x(e)$ inside the CRDRs of extreme starbursts dramatically alters the star-formation initial conditions relevant for the ambipolar-diffusion (AD) regulated star formation scenario. Indeed, the much larger ionization fractions that can now be achieved deep inside H_2 clouds can in principle: a) keep the magnetic field lines strongly “threaded” into molecular gas at much higher densities, and b) as a result render much of its mass incapable of star-formation, at least in the simple (AD)-regulated star formation scenario. This stems

from the now much longer ambipolar diffusion timescales: $\tau_{AD} \sim 1.6 \times 10^{14} x(e)$ yrs needed for a CR-ionized core with density $n(H_2)$ to lose magnetic flux and collapse ([20]). Indeed, after inserting $x(e)$ (from Eq. 1.6) it is:

$$\tau_{AD} = 3.2 \times 10^7 r_{gd} \left(\frac{n_{ch}}{2n(H_2)} \right)^{1/2} \times \left[\left(1 + \frac{n_{ch}}{8n(H_2)} \right)^{1/2} + \left(\frac{n_{ch}}{8n(H_2)} \right)^{1/2} \right] \text{ yrs.} \quad (1.9)$$

In Fig. 1.6 τ_{AD} is shown as a function of the CR ionization rate ζ_{CR} (assumed $\propto U_{CR}$) for three typical densities of cloud cores inside CRDRs. It is obvious that the much higher ζ_{CR} values expected in the CRDRs of (U)LIRGs will make the corresponding τ_{AD} timescales much longer than those expected in the Galaxy. Moreover τ_{AD} in (U)LIRGs will be longer than their so-called gas consumption timescales $\tau_{cons} = M(H_2)/SFR$, which are observationally determined using $M(H_2)$ (usually obtained via CO J=1–0) and the star formation rate (SFR) (usually obtained from L_{IR}).

For any theory of star formation τ_{cons} represents a natural *maximum* for any theoretically deduced characteristic star-formation timescale $\tau_{*,ch}$ since star-formation feedback (via SNR-induced shocks, O,B star far-UV radiation) will only lengthen any such $\tau_{*,ch}$ by destroying the H_2 clouds fueling star formation (which then have to reform to be SF-capable again). From Fig. 1.6 it is obvious that for (U)LIRGs it will always be $\tau_{AD} > \tau_{cons}$, thus rendering AD-regulated star formation as unrealistic. For the average ISM conditions in such vigorously star-forming galaxies a process such as reconnection diffusion ([36]) can still provide magnetic field diffusion fast enough as to keep $\tau_{*,ch} < \tau_{cons}$ ([37]).

In summary, in the AD-diffusion regulated star-formation scenario, as in the gravoturbulent one, *the large CR energy densities in the CRDRs of compact starbursts will dramatically alter the initial conditions for star formation.* The effects on the emergent stellar IMF are however less clear to discern than for gravoturbulently-regulated star formation, especially if fast reconnection diffusion plays a role in removing magnetic field support from dense H_2 gas with orders of magnitude larger ionization fractions than in ordinary star-forming galaxies.

1.4.2 CR-induced effects on the equation of state of the H_2 gas

Another effect of the large CR energy densities in the CRDRs of compact starbursts is *the erasing of the so-called inflection point of the effective equation of state (EOS) of the H_2 gas.* The latter, parametrized as a polytrope $P = K\rho^\gamma$, is used in many numerical simulations of self-gravitating turbulent gas. These found its polytropic index γ , and more specifically the so-called EOS inflection point (i.e. the characteristic density n_c where $\gamma < 1$ for $n < n_c$ flips to $\gamma \geq 1$ for $n \geq n_c$), playing a crucial role in de-

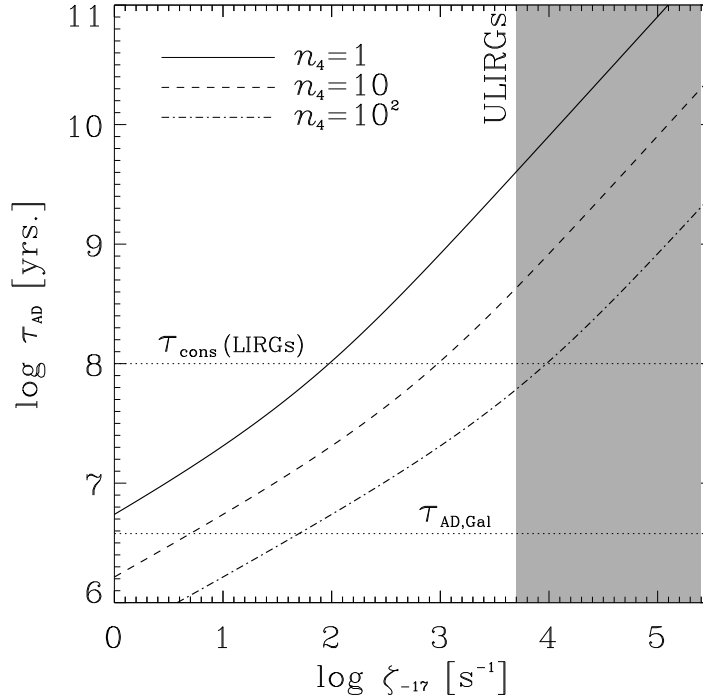


Fig. 1.6 The ambipolar diffusion (AD) timescale as a function of the CR ionization rate $\zeta_{-17} = \zeta_{\text{CR}} / (10^{-17} \text{ s}^{-1})$ (assumed $\propto U_{\text{CR}}$), for $n = [10^4, 10^5, 10^6] \text{ cm}^{-3}$ ($n_4 = n(\text{H}_2) / (10^4 \text{ cm}^{-3})$). For comparison the AD timescale for ISM conditions typical in the Galaxy is also shown as a horizontal line at the bottom. The H_2 gas consumption timescale $\tau_{\text{cons}} \sim M(\text{H}_2) / \text{SFR}$ for a typical (U)LIRG is also marked by the higher horizontal line. The shaded area marks the region where such galaxies are expected to be in terms of the ζ_{CR} in their CRDRs, where clearly $\tau_{\text{AD}} > \tau_{\text{cons}}$.

termining the functional shape and mass scale of the resulting mass spectrum of the collapsed dense gas cores (and thus the stellar IMF) ([38, 39]). For ordinary ISM conditions this inflection point occurs within CRDRs at $n_c \sim 10^5 \text{ cm}^{-3}$ ([22, 39]) because of the onset of strong thermal gas-dust coupling in the (far-UV)/optically-shielded gas regions, which makes them nearly isothermal and sets a characteristic IMF mass scale of $M_*^{(\text{ch})} \sim M_{\text{jeans}}(n_c)$.

In the CRDRs of compact starbursts the H_2 gas and the dust remain thermally decoupled with $T_{\text{kin}} > T_{\text{dust}}$ for densities as high as $n \sim 10^6 \text{ cm}^{-3}$ (Fig. 1.4), erasing the EOS inflection point. This maintains strong H_2 gas cooling ($\propto n^2$) at much higher densities ($\geq n_c$), rendering local cooling timescales (τ_{cool}) much shorter than the dynamical ones (τ_{dyn}). This allows thermodynamics to always stay a step ahead of self-gravity in decreasing the local Jeans mass (as densities climb and temperatures drop) faster than the gravitationally-driven evolution of the cloud fragments it to mass fragments of $\sim M_{\text{jeans}}(\mathbf{r}, t)$. A comparison of these two important timescales as a function of the CR energy densities is shown in Fig. 1.7, from where it be-

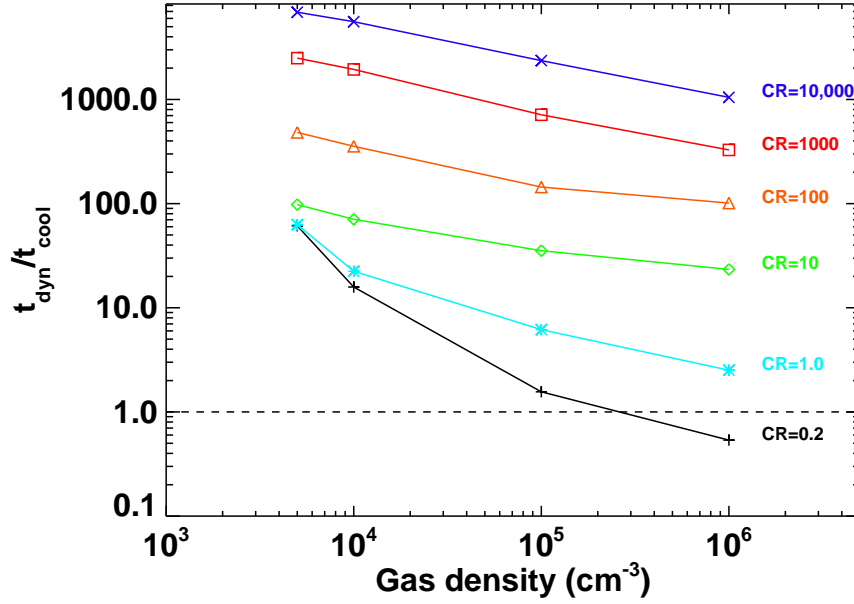


Fig. 1.7 The ratio of dynamical/cooling timescales for H₂ gas in CRDRs, for CR energy densities expected in star-formation-quiescent up to starburst galaxies (scaled to the average Galactic value).

comes obvious that an inflection point where $\tau_{\text{dyn}}/\tau_{\text{cool}} \sim 1$ is not even approached once $U_{\text{CR}}/U_{\text{CR,Gal}} \geq 10$, even for densities as high as $\sim 10^6 \text{ cm}^{-3}$. Clearly *any future numerical simulations of molecular clouds in extreme CRDRs must take this into account, or abandon the use of an EOS for the gas altogether.*

1.5 A CR-controlled stellar IMF: some consequences

A top-heavy stellar IMF can be the result a higher characteristic mass $M_{\text{ch}}^{(*)}$ for the young stars (the so-called IMF ‘knee’, which is $\sim (0.3-0.5) M_{\odot}$ for the Galaxy) or a shallower power law than its Salpeter value of $\alpha \sim 2.35$ (for an IMF functional form of $dN(M_*)/dM_* \propto M_*^{-\alpha}$ and stellar masses between $1 M_{\odot}$ and $100 M_{\odot}$). In a gravo-turbulent scenario the exact shape and mass scale of the emergent stellar IMF under the very different star formation initial conditions in extreme CRDRs of ULIRGs can only be determined with new H₂ cloud simulations that make use of these new conditions. In the past simulations using so-called starburst ISM conditions have been done, recovering large $M_{\text{ch}}^{(*)}$ in such environments ([40]). Unfortunately such simulations used conditions typical of PDRs rather than CRDRs, an approach that

would have then produced a varying IMF even in the Milky Way given the large range of gas properties in its PDRs. It was only recently that the effects of large CR energy densities on H_2 cloud fragmentation and the stellar IMF have been explored ([41]) and found $M_{ch}^{(*)}$ boosted to $\sim(2-3) M_\odot$ (Fig. 1.8).

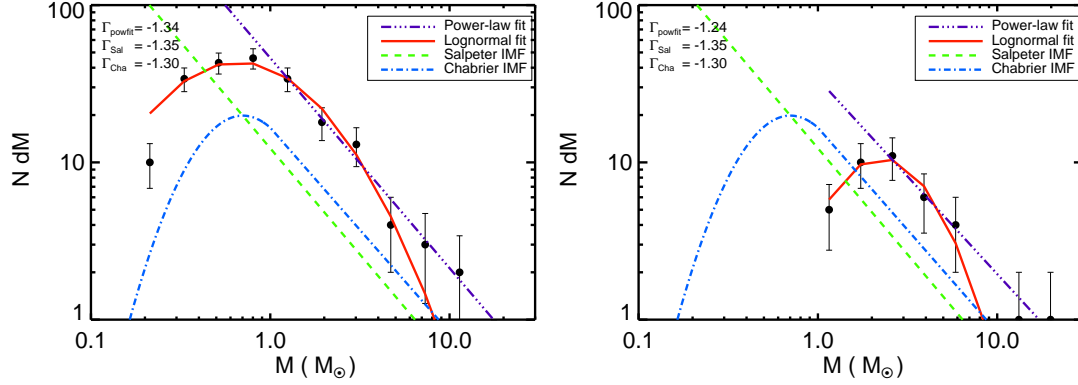


Fig. 1.8 The stellar initial mass functions (IMFs) from numerical simulations of turbulent H_2 clouds, for $U_{CR}=U_{CR,Gal}$ (left), $100 \times U_{CR,Gal}$ (right) [41]. For comparison purposes, a Salpeter-type (green dashed) and Chabrier-type (blue dot-dashed) IMF fits to the emergent mass spectrum are also shown along with a linear fit and a lognormal fit (purple and red lines). The power-law slopes above the turn-over mass $M_{ch}^{(*)}$ are given in the upper left corner.

The dependance of the thermal and ionization state of the gas in CRDRs on the average U_{CR} permeating the ISM of a galaxy naturally links the SF initial conditions and the resulting IMF to the average SFR density $\dot{\rho}_{sfr}$, provided $U_{CR} \propto \dot{\rho}_{sfr}$ (with the details of CR transport/escape mechanisms in quiescent SF disks and starbursts setting the proportionality factor). CR-controlled star formation initial conditions then naturally yield a bimodal stellar IMF in galaxies, with high values of $\dot{\rho}_{sfr}$ determining the branching point, namely:

(merger-driven star formation) \rightarrow (high $\dot{\rho}_{sfr}$) \rightarrow (high U_{CR}) \rightarrow (top heavy IMF),
 (isolated gas-rich disk star formation) \rightarrow (low $\dot{\rho}_{sfr}$) \rightarrow (low U_{CR}) \rightarrow (Galactic IMF).

Such an IMF bimodality, with a top-heavy IMF in merger/starbursts versus a regular IMF in isolated gas-rich disks has been postulated for some time in hierarchical galaxy formation models seeking to explain their relative populations across cosmic time in Λ CDM cosmologies ([42]). *CR-controlled star formation initial conditions in galaxies can now set this on a firm physical basis for the first time.* It must be noted that a top-heavy IMF in high- $\dot{\rho}_{sfr}$ systems such as compact starbursts in mergers, will also have serious implications on the SFRs deduced from their observed IR luminosities as such IMFs will have several times higher energy outputs per stellar mass than the ordinary one. Then the tremendous SFRs deduced

for merger/starbursts, especially at high redshifts ($\sim 10^3 \text{ M}_\odot \text{ yr}^{-1}$), may actually be $\sim(3-5)$ times lower.

Finally an $\dot{\rho}_{sfr}$ -dependant IMF as the outcome of CR-controlled star formation initial conditions in galaxies will also naturally yield integrated galactic IMFs (IGIMFs) that depend on the star formation history (SFH) of galaxies. This is simply because $\dot{\rho}_{sfr}$ can change significantly during the evolutionary track of a galaxy, especially during its early gas-rich epoch, even in the absence of mergers. Such a SFH-dependance of the IGIMFs has been considered as the cause behind the well-known mass-metallicity relation of galaxies ([43]).

1.6 Future outlook

The unique signatures imparted on the thermal and chemical state of the H_2 gas in extreme CRDRs have now been studied extensively ([29, 44, 45]), and most of them will be easily accessible in the new era of ALMA whose commissioning is now ongoing at Llano de Chajnantor on the Atacama Desert Plateau. Numerical studies of H_2 clouds without the use of an EOS for the gas, that take also into account the strongly anchored magnetic fields on dense gas with large ionization fractions are now becoming possible. High-energy γ -ray observations now started directly probing the average CR energy densities of other galaxies ([46, 47]). Thus we are looking at a decade where the properties of CRDRs, their effect on the stellar IMF of galaxies, and their role in galaxy formation can be decisively explored with powerful theoretical and observational tools. Finally these explorations will critically benefit from studies of the stellar IMF and its dependence on ambient conditions in galaxies that are now converging to much sharper picture ([48]).

Acknowledgements Padelis P. Papadopoulos would like to warmly thank the organizers of the conference in Sant Cugat for an exciting week where much was learned and new vistas for both high energy and the so-called low energy Astrophysics came into view. This project was also funded by the John Latsis Public Benefit Foundation. The sole responsibility for the content lies with its authors.

Appendix

The CR heating rate used in this work is given by

$$\Gamma_{\text{CR}} = 1.95 \times 10^{-28} n_{\text{H}} \left(\frac{\zeta_{\text{CR}}}{1.3 \times 10^{-17} \text{ s}^{-1}} \right) \text{ ergs cm}^{-3} \text{ s}^{-1} \quad (1.10)$$

where $\zeta_{\text{CR}} \propto U_{\text{CR}}$ being the Cosmic Ray ionization rate (in s^{-1}), with an adopted Galactic value of $\zeta_{\text{CR,Gal}} = 5 \times 10^{-17} \text{ s}^{-1}$ (corresponding to $U_{\text{CR}} = U_{\text{CR,Gal}}$), and $n_{\text{H}} = 2n(\text{H}_2)$ for fully molecular gas. For an optically thin OI line (and thus maximal cooling) $\Lambda_{\text{OI63}} = \chi_{\text{O}} n_{\text{H}} C_{\text{ul}} E_{\text{ul}}$, which becomes

$$\Lambda_{\text{OI63}} = 3.14 \times 10^{-14} \chi_{\text{O}} n_{\text{H}} C_{\text{ul}} \left(\frac{g_{\text{u}}}{g_{\text{l}}} \right) \exp(-227.72/T_{\text{kin}}) \text{ ergs} \quad (1.11)$$

where $g_{\text{u}}=3$ and $g_{\text{l}}=5$, and $\chi_{\text{O}}=[\text{O}/\text{H}]$ being the abundance of oxygen not locked onto CO ($\chi_{\text{O}} \sim 4.89 \times 10^{-4}$). The collisional de-excitation coefficient is given by ([16])

$$C_{\text{ul}} = n_{\text{H}} 10^{0.32 \log T_{\text{kin}} - 10.52} = 3.02 \times 10^{-11} n_{\text{H}} T_{\text{kin}}^{0.32} \text{ cm}^{-3} \text{ s}^{-1}, \quad (1.12)$$

Thus finally Equation 1.11 becomes,

$$\Lambda_{\text{OI63}} = 2.78 \times 10^{-28} n_{\text{H}}^2 T_{\text{kin}}^{0.32} \exp(-227.72/T_{\text{kin}}) \text{ ergs cm}^{-3} \text{ s}^{-1}. \quad (1.13)$$

For densities of $n_{\text{H}} < 10^5 \text{ cm}^{-3}$ and strong CR fluxes, a small fraction of carbon remains in the form of C^+ , acting as a coolant with

$$\Lambda_{\text{C}^+} = 1.975 \times 10^{-23} n_{\text{H}}^2 \chi_{\text{C}^+} \exp(-92.2/T_{\text{kin}}) \text{ ergs cm}^{-3} \text{ s}^{-1}, \quad (1.14)$$

computed in a similar fashion as the OI(63 μm) line cooling, and for a fully transparent medium. Gas-grain accommodation cooling the gas depending on their temperature difference can be expressed as ([17]):

$$\Lambda_{\text{g-d}} = 4.0 \times 10^{-12} \alpha n_{\text{H}} n_{\text{d}} \sigma_{\text{g}} \sqrt{T_{\text{kin}}} (T_{\text{kin}} - T_{\text{dust}}) \quad (1.15)$$

where n_{g} is the number density of dust grains and σ_{g} is the grain cross-section (cm^2). If the gas-to-dust ratio is 100, the dust mass density is $\rho_{\text{d}} = 3.5 \text{ g cm}^{-3}$, and a dust radius of $a = 0.1 \mu\text{m}$ then

$$n_{\text{d}} = 2.2 \times 10^{-2} \times \mu_{\text{H}} n_{\text{H}} / (4/3 \pi \rho_{\text{d}} a^3) = 7.88 \times 10^{-12} n_{\text{H}}. \quad (1.16)$$

The gas-grain accommodation factor α is given by ([18]):

$$\alpha = 0.35 \exp \left(-\sqrt{\frac{T_{\text{dust}} + T_{\text{kin}}}{500}} \right), \quad (1.17)$$

which we set to the maximum value $\alpha=0.35$ (i.e. maximum gas cooling from gas-dust interaction). Thus the cooling term due to the gas-dust interaction (Equation 1.15) becomes

$$\Lambda_{g-d} = 3.47 \times 10^{-33} n_H^2 \sqrt{T_{\text{kin}}} (T_{\text{kin}} - T_{\text{dust}}) \text{ ergs cm}^{-3} \text{ s}^{-1}. \quad (1.18)$$

Finally detailed PDR code models allow us to parametrize the cooling due to the CO rotational transitions as

$$\Lambda_{\text{CO}} = 4.4 \times 10^{-24} \left(\frac{n_H}{10^4 \text{ cm}^{-3}} \right)^{3/2} \left(\frac{T_{\text{kin}}}{10 \text{ K}} \right)^2 \left(\frac{\chi_{\text{CO}}}{\chi_{[\text{C}]}} \right) \text{ ergs cm}^{-3} \text{ s}^{-1}, \quad (1.19)$$

where we set $\chi_{\text{CO}}/\chi_{[\text{C}]}=(0.97, 0.98, 0.99, 1.0)$ for densities of 5×10^3 , 10^4 , 10^5 , 10^6 cm^{-3} respectively (with $\chi_{\text{CO}}/\chi_{[\text{C}]}=1$ corresponding to all carbon locked onto CO).

References

1. Hollenbach D. J., & Tielens A. G. G. M. Reviews of Modern Physics **Vol. 17**, No1, January 1999
2. Wolfire M. G., McKee C. F., Hollenbach D., Tielens, A. G. G. M. 2003, Astrophysical Journal, **587**, 278
3. Tielens A. G. G. M. & Hollenbach D. J. 1985a Astrophysical Journal, **291**, 722
4. Tielens A. G. G. M. & Hollenbach D. J. 1985b Astrophysical Journal, **291**, 747
5. Gao Yu, & Solomon P. M. 2004, Astrophysical Journal Supplement, **152**, 63
6. Solomon P. M., Downes D., & Radford S. J. E 1992, Astrophysical Journal Letters **387**, 55
7. Padoan P., & Nordlund A. 2002, Astrophysical Journal, **576**, 870
8. Pan L., & Padoan P. 2009, Astrophysical Journal, **692**, 594
9. Pelupessy F. I., Papadopoulos P. P., & van der Werf P. P. 2006, Astrophysical Journal, **645**, 1024
10. Bergin, E. A. & Tafalla, M. 2007, Annual Reviews of Astronomy & Astrophysics, **45**, 339
11. Pineda, J. L. & Bensch, F. 2007, Astronomy & Astrophysics, **470**, 615
12. Pineda, J. E., Goodman, A. A., Arce, H. E. et al. 2010, Astrophysical Journal Letters, **712**, L116
13. Goldsmith, P. F., & Langer, W. D. 1978, Astrophysical Journal, **222**, 881

14. Ossenkopf, V. 2002, *Astronomy & Astrophysics*, **391**, 295
15. Goldsmith, P. F. 2001, *Astrophysical Journal*, **557**, 736
16. Liseau, R. et al. 1999, *Astronomy & Astrophysics* 1999, **344**, 342
17. Burke, J. R., & Hollenbach, D. J. 1983, *Astrophysical Journal*, **265**, 223
18. Groenewegen, M. A. T. 1994, *Astronomy & Astrophysics*, **290**, 531
19. Papadopoulos, P. P., Thi. W.-F., Miniati, F., & Viti S. 2011, *Monthly Notices of the Royal Astronomical Society*, **414**, 1705
20. McKee, C. F. 1989, *Astrophysical Journal*, 1989, *Astrophysical Journal*, **345**, 342
21. Mouschovias, T. Ch., & Spitzer L. Jr, 1976, *Astrophysical Journal*, **210**, 326
22. Larson, R. B. 2005, *Monthly Notices of the Royal Astronomical Society*, **359**, 211
23. Elmegreen B. G., Klessen R. S., & Wilson C. D. 2008, *Astrophysical Journal*, **681**, 365
24. Sakamoto, K. et al. 2008, *Astrophysical Journal*, **684**, 957
25. Downes D., & Solomon P. M. 1998, *Astrophysical Journal*, **507**, 615
26. Greve T. R., Papadopoulos P. P., Gao Y., & Radford S. J. E. 2009, *Astrophysical Journal*, **692**, 1432
27. Papadopoulos P. P., van der Werf P. P., Xilouris E. M., Isaak K. G., Gao Y., & Muehle S. 2012, *Monthly Notices of the Royal Astronomical Society*, (in press, arXiv:1109.4176)
28. Rangwala N. et al. 2012, *Astrophysical Journal*, **743**, 94
29. Papadopoulos P. P., 2010, *Astrophysical Journal*, **720**, 226
30. Yusef-Zadeh F., Wardle M., Roy S. 2007, *Astrophysical Journal Letters* **665**, L123
31. Bradford C. M., Nikola T., & Stacey G. J. 2003, *Astrophysical Journal* **586**, 891
32. Hailey-Dunsheath S., Nikola T., Stacey G. J. et al. 2008, *Astrophysical Journal Letters*, **689**, L109
33. Klessen R. S. 2004, *Astrophysics and Space Science*, **292**, Issue 1, p. 215
34. Elmegreen B. G., Klessen R. S., & Wilson C. D. 2008, *Astrophysical Journal*, **681**, 365
35. Elmegreen B. G. 1989, *Astrophysical Journal*, **338**, 178
36. Lazarian A. 2011, *Nonlin. Processes Geophys.* (in press, arXiv:1111.0694)
37. Lazarian A. Esquivel A., & Crutcher R. 2012, *Astrophysical Journal* (arXiv:1206.4698)
38. Li Y., Klessen R. S., & McLow M.-M. 2003, *Astrophysical Journal*, **592**, 975

39. Jappsen A.-K., Klessen R. S., Larson R. B., Li Y., McLow M.-M. 2005, *Astronomy & Astrophysics*, **435**, 611
40. Klessen R. S., Spaans M. & Jappsen A.-K. 2007, *Monthly Notices of the Royal Astronomical Society*, **374**, L29
41. Hocuk S., & Spaans M. 2011, *Astronomy & Astrophysics*, **536**, 41
42. Baugh C. M. et al. 2005, *Monthly Notices of the Royal Astronomical Society*, **356**, 1191
43. Koeppen J., Weidner C., & Kroupa P. 2007, *Monthly Notices of the Royal Astronomical Society*, **375**, 673
44. Meijerink R., Spaans M., Loenen A. F., & van der Werf P. P. 2011, *Astronomy & Astrophysics*, **525**, 119
45. Bayet E., Williams D. A., Hartquist T. W., & Viti S. 2011, *Monthly Notices of the Royal Astronomical Society*, **414**, 1583
46. Acciari V. A. et al. 2009, *Nature*, **462**, 770
47. Acero F. et al. 2009, *Science*, **326**, 1080
48. Kroupa P. et al. 2012, in *Stellar Systems and Galactic Structure*, Vol. V. (in press, arXiv:1112.3340)